Simultaneous 280 MHz EPR Imaging of Rat Organs During Nitroxide Free Radical Clearance

M. Alecci, M. Ferrari, V. Quaresima, A. Sotgiu, and C. L. Ursini
Dipartimento di Scienze e Tecnologie Biomediche, Universita' dell'Aquila, Coppito, 67100-L'Aquila, Italy

ABSTRACT A radio frequency (RF) (280 MHz) electron paramagnetic resonance (EPR) spectroscopy and imaging apparatus has been used to localize a pyrrolidine nitroxide free radical in the rat abdomen and thorax. The nitroxide 2,2,5,5,-tetramethylpyrrolidine-1-oxyl-3-carboxylic acid (PCA) had a whole body monoexponential decay with half-life of 13.3 ± 0.7 (n = 4), 19.4 ± 0.2 (n = 3), and 23 ± 2 (n = 6) min for 1, 2, and 3 mmol/kg PCA, respectively. Up to seven one-dimensional longitudinal projections were collected on six rats in the presence of a 8 mT/m field gradient. With an injection dose of 3 mmol/kg, PCA half-lives were 19 ± 1, 17 ± 2, and 22 ± 2 min (n = 6) in the lower abdomen, in the liver, and in the thorax, respectively. Thorax half-life was significantly longer than liver half-life. Sequential two-dimensional images of PCA distribution in a plane longitudinal to the rat body were obtained from eight spectra in the presence of a gradient of 12 mT/m (acquisition time 5 min; spatial resolution 8 mm). After 7 min, the nitroxide was detectable in the left side of the thorax area, but it was mostly localized in the liver. PCA was more uniformly distributed in the image collected after 17 min.

INTRODUCTION

Low frequency EPR spectroscopy allows the detection of paramagnetic species in small laboratory animals. EPR admits the attractive possibility of determining the in vivo oxygen concentration by measuring the local concentrations of exogenous paramagnetic species, such as nitroxide free radicals, at different times (Swartz and Glockner, 1991). Experiments are usually performed at L-band (1–2 GHz). The addition of field gradients and reconstruction techniques enables the distribution of the free radicals in the tissues to be mapped (Colacicchi et al., 1992; Ohno et al., 1991).

Until now, no attempts have been made to study the nitroxide distribution in different organs of the whole rat simultaneously. The literature on the distribution of nitroxides has been limited to EPR spectroscopy and/or imaging of small biological samples at X- or L-band. The amount of nitroxide concentration in the mouse liver region was obtained at L-band by an EPR spectrometer equipped with a surface coil 1 cm in diameter (Bacic et al., 1989). The use of surface coils is appropriate when EPR spectroscopy is limited to subcutaneous tissues (about 0.8 cm) near the surface loop. This is because the sensitivity of the surface coil reflects the spatial profile of the microwave field along its axis. The use of loop-gap (Froncisz et al., 1982) or re-entrant (Sotgiu, 1985) resonators allows the observation of the signal from the whole sample when it is positioned in the central region of the resonator. A 2-D EPR image of a growing melanoma tumor implanted into a mouse tail was obtained using a loop-gap resonator operating at 1.56 GHz (Berliner et al., 1987). Despite the low resolution and the long acquisition time (10 min), a necrotic region was found in the center of the image. The first three-dimensional image of a rat tail was obtained in 25 min operating at 1.2 GHz (Alecci et al., 1990). The low resolution image was capable of resolving the tail vascular structure. More recently, high quality L-band EPR images of a rat head and a mouse lung were obtained. Head images, collected in 40 min, showed a nitroxide-deficient area corresponding to the brain (Ishida et al., 1992). Post mortem 2-D images of the mouse lung were obtained by filling the bronchial tree with a nitroxide free radical (Takeshita et al., 1991).

The use of L-band frequencies allows the detection of the signal only from a small region of the sample (1–3 cm). To obtain the distribution of the nitroxide in larger samples, it is necessary to work at RF and to design suitable resonators. Our laboratory developed an EPR imaging (EPRI) spectrometer that operates at 280 MHz and allows the observation of laboratory animals of up to 150 g (Alecci et al., 1992a). Using this instrument with a temperature control system, we were able to study the PCA pharmacokinetics in whole rats (50–60 g) and to obtain transversal 2-D images in 6 min (Quaresima et al., 1992).

In this study, the sensitivity of the loop-gap resonator along its longitudinal axis has been determined in order to obtain a correct spatial distribution in in vivo experiments. The EPRI apparatus has been utilized to investigate: (1) regional PCA distribution along the axis of the rat during the reduction/clearance phase; (2) the simultaneous study of the PCA reduction in the lower abdomen, liver, and thorax and the contribution of these regions to the whole body PCA

Received for publication 13 October 1993 and in final form 9 June 1994.
Address reprint requests to Dr. M. Alecci, Dipartimento di Scienze e Tecnologie Biomediche, Universita' dell'Aquila, Coppito, 67100-L'Aquila, Italy. Tel.: 011-39-862-433493; Fax: 011-39-862-433433; E-mail: sotgiu@vxscaq.aquila.infn.it.

Abbreviations used: DPPH, 2,2-diphenyl-1-picrylhydrazylhydrate powder; EPR, electron paramagnetic resonance; EPRI, EPR imaging; f_o, resonator frequency; H, RF magnetic field; H_m, modulation field; PCA, 2,2,5,5,-tetramethylpyrrolidine-1-oxyl-3-carboxylic acid; Q, resonator quality factor; RF, radio frequency; 1-D, one-dimensional; 2-D, two-dimensional.

0006-3495/94/09/1274/06 $2.00

metabolism; (3) the 2-D spatial distribution of PCA along the axis of the whole rat at two different times during the PCA reduction/clearance phase.

MATERIALS AND METHODS

Radio frequency measurements

The description of the whole EPRI apparatus is given elsewhere (Alecci et al., 1992b). In this study, a one loop-two gap resonator 7 cm in external diameter, 1 cm in wall thickness, and 10 cm in length was utilized. The loop was obtained by the use of adhesive copper tape applied to the external surface of a teflon tube. The two gaps were filled by teflon sheets 0.4 mm thick. The resonator frequency (f_o) could be varied in the range 250–350 MHz by using sheets of different sizes. The quality factor (Q) of the empty resonator, measured as previously described (Alecci et al., 1992b), was 1086 at f_o = 304 MHz.

Signal intensity is determined by the combined effect of the RF magnetic field (H_1) and the modulation field (H_m). However, the geometrical dimensions of the modulation coils are much larger than those of the observed region (Alecci et al., 1992b), and this ensures the homogeneity of H_m. Moreover, the low frequency (8.3 kHz) value of H_m makes distortion of the field caused by the sample unlikely. To obtain a correct in vivo spin probe spatial distribution, a careful characterization of H_1 inside the resonator is required. A fast and accurate EPRI technique to measure H_1 along the axial dimension of the resonator uses a stable paramagnetic sample of well defined shape and concentration (Lebedev and Yakimchenko, 1991; Marshall et al., 1988; Ogata et al., 1992). The EPR spectrum $s(z)$ is then recorded in the presence of a linear field gradient and represents the convolution between the zero-gradient line shape $g(z)$ and the projection $p(z)$ of the spin density of the sample along the direction of the field gradient, i.e.,

$$s(z) = \int_{-\infty}^{+\infty} p(z')\, g(z - z')\, dz'. \quad (1)$$

The projection $p(z)$ can be calculated by deconvolution in the Fourier space (Momo et al., 1993) and is correlated with the sample spin density $r(x, y, z)$ by the equation

$$p(z) = \int_{-\infty}^{+\infty} \int_{-\infty}^{+\infty} n(x, y, z)\, r(x, y, z)\, dx\, dy, \quad (2)$$

where the integral is evaluated in the planes perpendicular to the z gradient; $n(x, y, z)$ is a sensitivity distribution function that depends on H_1. In the present case, the spin density is constant and any variation of $p(z)$ must be attributed to an uneven distribution of H_1 along the z axis. Because the sensitivity distribution function in a central region of the resonator of 2.5 cm in diameter can be considered independent of the radial coordinate (Alecci et al., 1992b) and proportional to H_1^2 (Dalal et al., 1981), we obtain from Eq. 2 that $H_1(z) = k\sqrt{p(z)}$, where k is a constant that depends on the spin density.

Experimentally, the $H_1(z)$ distribution in a rat was simulated by a cylinder (2.8 cm in diameter, 10 cm in length) containing 1 mM PCA (Aldrich Chemical Co., Milwaukee, WI) solution. The effect of the solution conductivity on $H_1(z)$ was determined using three different solutions of PCA: in deionized water (Q = 770, f_o = 298 MHz), in 35% physiological saline solution (Q = 268, f_o = 299 MHz), and in physiological saline solution (Q = 114, f = 301 MHz). $H_1(z)$, at six positions on the axis of the empty resonator, was also investigated by measuring the intensity of the EPR signal of a small cylinder (0.8 cm in diameter, 0.5 cm in length) containing 2,2-diphenyl-1-picryl-hydrazylhydrate (DPPH, Aldrich Chemical Co., Milwaukee, WI) powder (Fig. 1). Because of the small dimensions of the cylinder containing the PCA compared with the wavelength of the RF field, this phantom adequately represents a biological sample (Gadian and Robinson, 1979; Hoult and Lauterbur, 1979). The presence in the resonator of different regions with higher conductivity will reduce the Q and, as a consequence, the intensity of the RF field H_1 everywhere in the sample.

In vivo spectroscopy

For EPR spectroscopy and imaging purposes, n = 15 male Wistar rats (45–65 g) were anesthetized with Ethyl Carbamate, (Sigma-Aldrich Chemical Co.) (1 g/kg, i.p.). The jugular vein and the carotid artery were cannulated, respectively, for PCA injection and blood pressure recording. The rats received an intravenous bolus of PCA in physiological saline solution buffered to pH 7.4. To achieve the final concentration of 1, 2, 3, and 4 mmol/kg, in the 50-g rat, 0.33 ml (injection time 15 s), 0.66 ml (injection time 30 s), 1.00 ml (injection time 60 s), and 1.33 ml (injection time 75 s) of 150 mM PCA solution were injected, respectively. During PCA injection, blood pressure increased 10–20 mmHg and recovered to the baseline values in 2–4 min. PCA is a partially ionized negative nitroxide free radical that can cross the cell membranes and was chosen because of its low toxicity (LD_{50} = 15 mmol/kg) and its relatively long half-life (Quaresima et al., 1992). Body temperature was monitored by a rectal thermometer and maintained at 38°C by a water jacket inserted in the resonator. The rats were placed into the loop-gap resonator in a supine position; the tail, the bladder region, and the head were outside the active region of the resonator. The acquisition parameters of the EPR spectra were: center field 8.3 mT; scan range 2.2 mT; scan time 25–50 s; time constant 300 ms; RF power 110 mW; frequency field modulation 8.6 kHz; and modulation amplitude 0.04 mT. The in vivo PCA spectrum did not show significant line broadening. To decrease the acquisition time, only the low field peak of the PCA triplet was recorded. The sensitivity of the present apparatus was 10 μM with aqueous phantoms (Alecci et al., 1992b). The in vivo lowest detectable PCA concentration (signal-to-noise ratio = 2) without gradients was approximately 44 μM (Quaresima et al., 1992). This does not represent an ultimate sensitivity for continuous wave apparatus working at this frequency, but depends on the bandwidth of the apparatus. In fact, our instrument can work at any frequency between 200 MHz and 1 GHz simply by changing the sample resonator (Alecci et al., 1992b). A different approach, based on a quartz controlled source, has shown a better sensitivity with aqueous samples (Brivati et al., 1991).

In vivo imaging

The use of a 1-D longitudinal gradient allowed the measurement of the PCA distribution along the axis of the rat. To prevent overlapping of the PCA hyperfine components, a maximum field gradient value of 12 mT/m was used. The spatial resolution depends mainly on the signal-to-noise ratio, the gradient intensity and the PCA linewidth (0.14 mT). The maximum achievable spatial resolution from our EPRI apparatus was 10 mm. The use of a Fourier deconvolution technique (Momo et al., 1993) made it possible to increase the resolution to 8 mm. In in vivo experiments, to assign the different regions to specific organs, a cylinder (0.8 cm in diameter, 1.5 cm in length) containing DPPH powder was positioned transversely on the area of the rat's abdomen corresponding to the liver. The DPPH positioning was standardized taking into account that, on 48–52 g rats, the nose-center of the liver distance was 69 mm and the liver maximal dimension along the axis of the animal was 16 mm. The accuracy of the correspondence between the DPPH reference and the center of the liver was about 3 mm, taking into account the respiratory movements and some biological variability of the liver size. This correspondence was verified post mortem. The DPPH spectra were obtained at the beginning of the experiment with and without gradient to obtain the axial projection of the DPPH reference. The maximum value of the DPPH projection enables localization of the center of the liver (Fig. 2). The accuracy of this localization (about 2 mm) depends on the DPPH linewidth (0.16 mT) and the value of the gradient (25 mT/m). Taking into account that the upper poles of the kidneys overlap the lower part of the liver, the dimension of the liver along the axis of the animal was restricted to 14 mm. This made it possible to assign the PCA signal to three regions: the lower abdomen, the liver, and the thorax. The PCA from these regions was quantified by evaluating the corresponding area under the 1-D spin density function.

To obtain PCA half-life, the EPR signal from whole body and localized regions was plotted on a semilogarithmic scale. Least-square linear regression analysis made it possible to calculate the half-lives, half-lives SEs, and

correlation coefficients (R^2). The R^2 was 0.94–0.99 for the whole body regressions (n = 15) and 0.81–0.98 for the three regions regressions (n = 6). These last correlation values were lower because of: a) the reduced signal-to-noise ratio of the spectra obtained with gradients; and b) the deconvolution technique that introduced additional noise. Differences among the half-lives of the three regions were calculated using Student's t-test with the Bonferroni correction for multiple comparison. All values are given as means ± SEM, and statistical significance was set at $p < 0.05$.

To obtain a true 2-D image, during the acquisition of the required projections, the PCA reduction has to be negligible. In practice in in vivo experiments, the above condition could be satisfied if the acquisition time was less than 5–8 min. 2-D images of the PCA distribution in a plane longitudinal to the rat body were obtained from eight spectra at angular increments of 22.5° in the presence of a gradient of 12 mT/m. The total acquisition time was 5 min. The 2-D images were calculated by a Fourier reconstruction technique (Alecci et al., 1992a). It is well known that in vitro the blood does not show any PCA-reducing activity (Bennett et al., 1990). Recent in vivo measurements, performed at X-band (9.5 GHz), have shown that after PCA injection the nitroxide reduction in the rat's circulating blood has a fast distribution phase of 3–4 min, followed by a slow reduction/clearance phase (Quaresima et al., 1993). The PCA half-life of this slow phase depends on the injected dose and it is similar to the whole rat half-life (Alecci et al., 1992c). The 5 min required for the acquisition of the projections did not allow us to obtain 2-D images during the distribution phase of PCA. However, we were able to acquire two sequential 2-D longitudinal images during the PCA slow reduction/clearance phase. To compare the PCA signal in 2-D images at different times, each image was scaled by a normalization factor obtained from the zero gradient spectrum recorded before the acquisition of the 2-D image.

Experiments were conducted using one of the following protocols: 1) PCA clearance at three different doses (1, 2, and 3 mmol/kg); 2) PCA administration (3 mmol/kg) for 1-D projections; 3) PCA administration (4 mmol/kg) for 2-D imaging.

RESULTS

Fig. 1 shows that $H_1(z)$ did not depend on sample conductivity and presented a consistent decrease only at the edges of the resonator axis. The $H_1(z)$ distribution is slightly asymmetric because of the presence of the inductive coupling loop of the same diameter as that of the resonator. Despite this, the EPR signal of a 1 mM PCA solution could be detected in the whole length of the resonator and H_1 variation was less than 20% in a central region of 5.5 cm. These data allowed us to obtain longitudinal images with negligible distortion and to measure the EPR signal from distinct regions of the resonator at different times.

To choose the nitroxide doses suitable for acquiring 2-D images, three PCA concentrations were tested. Whole body rat PCA reduction followed a monoexponential decay. PCA half-lives were 13.3 ± 0.7 (n = 4), 19.4 ± 0.2 (n = 3), and 23 ± 2 (n = 6) min for 1, 2, and 3 mmol/kg PCA, respectively. Therefore, to maintain the spin density relatively constant during acquisition, the highest PCA doses must be chosen for the 2-D images. It was possible to collect up to seven 1-D longitudinal projections during PCA reduction every 2–3 min. Fig. 2 shows a typical 1-D spin density distribution along the rat body at four different times of the reduction. A DPPH reference, positioned on the liver area in the presence of a longitudinal gradient, made it possible to assign the PCA signal to three regions: the lower abdomen, the liver, and the thorax. The nitroxide reduction followed a monoexponential decay in the three regions (Fig. 3). The PCA half-lives were 19 ± 1, 17 ± 2, and 22 ± 2 min (n = 6) in the lower abdomen, in the liver, and in the thorax, respectively, for 3 mmol/kg PCA. Thorax half-life was significantly longer than liver half-life.

Sequential longitudinal 2-D images were obtained from two animals. The first image (Fig. 4 *A*) showed that after 7 min the nitroxide was detectable in the left side of the thorax area, but it was mostly localized in the liver region. PCA was more uniformly distributed in the second image (Fig. 4 *B*) collected after 17 min.

DISCUSSION

Various EPRI instruments operating at L-band have been used to obtain 2-D images from localized regions of small laboratory animals. In these studies, the long acquisition time and the small size of the resonators prevented the mapping of the free radicals in different organs simultaneously (Alecci et al., 1990; Bacic et al., 1989; Berliner et al., 1987; Ishida

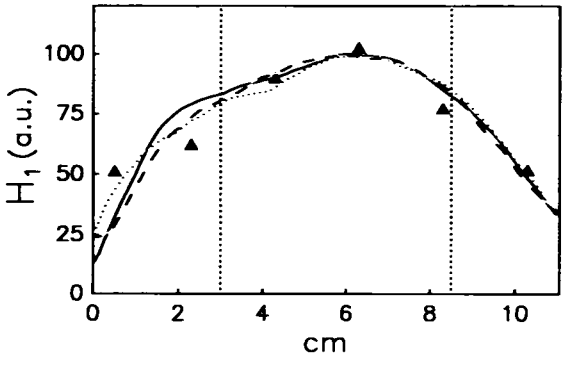

FIGURE 1 RF magnetic field (H_1) calibration along the axis of the loop-gap resonator obtained with a cylindrical phantom containing 1 mM PCA solution in: deionized water (——); 35% saline solution (· · · ·); and saline solution (---). The triangles correspond to H_1 on the axis of the empty resonator obtained with a small DPPH reference. Data are normalized for graphical purposes only. The vertical dashed lines indicate the central region of the resonator where the H_1 variation is less than 20%.

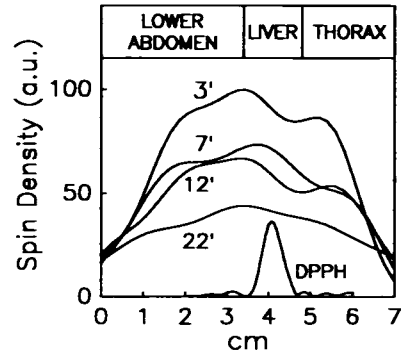

FIGURE 2 1-D PCA distribution along the longitudinal axis of a rat (52 g) obtained at different times after injection (3 mmol/kg). The three regions were assigned by the use of a DPPH reference positioned on the area of the rat's abdomen corresponding to the center of the liver. The acquisition time for each projection was 50 s.

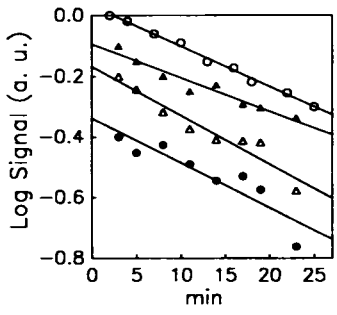

FIGURE 3 Representative PCA reduction (3 mmol/kg) from the whole body (○), thorax (▲), liver (△), and lower abdomen (●) regions of a 48-g rat. Corresponding half-lives ± SE (min) and regression coefficients (R^2) were 22.8 ± 0.7 and 0.99, 27 ± 3 and 0.94, 19 ± 2 and 0.92, and 20 ± 4 and 0.83. Solid lines represent the least-square linear regression fitting.

et al., 1992; Takeshita 1991). EPRI instruments operating in the RF range, as well as appropriate resonators, have been developed recently but have never been tested on laboratory animals (Brivati et al., 1991, 1993; Halpern et al., 1989), except to obtain preliminary 1-D spectral-spatial data on a mouse (Halpern et al., 1991).

In this paper, we report for the first time whole rat 2-D longitudinal images of PCA and its measurement at different times in the thorax and abdomen. The PCA dose (4 mmol/kg) was comparable with the doses of other EPRI studies (Ishida et al., 1992; Takeshita et al., 1991). The use of a DPPH reference allowed us to localize the liver with an accuracy of about 3 mm. The details of PCA biodistribution are not yet precisely known. Recently, we found that blood PCA concentration declines by 50% within 5 min of administration (Quaresima et al., 1993). On the first passage through the capillary bed, circulating PCA diffuses from the blood into the extravascular compartment. At the same time, kidney glomerular filtration contributes to a rapidly declining blood concentration (Couet et al. 1984). Previous experiments have shown greater reducing activity in the homogenates of the liver or kidney than in those of the brain, lung, heart, or muscle (Couet et al., 1984; Iannone et al., 1990). These in vitro tests of PCA reduction suggest the intriguing possibility that tissue differences in the rate of reduction can form a basis for differential enhancement. In our in vivo model, rat liver half-life was found to be significantly shorter than thorax half-life. The first 2-D image (Fig. 4 *A*) clearly indicated that most of the injected nitroxide was localized in the liver a few minutes after the injection. The left side of the thorax was also enhanced, suggesting a significant presence of PCA in the heart cavities. The mechanism for this hepatocyte uptake has been shown to be through a relatively nonspecific receptor known as the hepatocyte anion transporter (Grodd et al., 1987). It is thought that the physiological role of this receptor is to eliminate noxious anionic substances such as PCA from the body. The nitroxide was distributed more uniformly in the second image (Fig. 4 *B*) collected after 17 min. This image suggests an enhancement of the lungs. The low spatial resolution of our apparatus in the longitudinal projections does not allow the separation of the kidneys from the

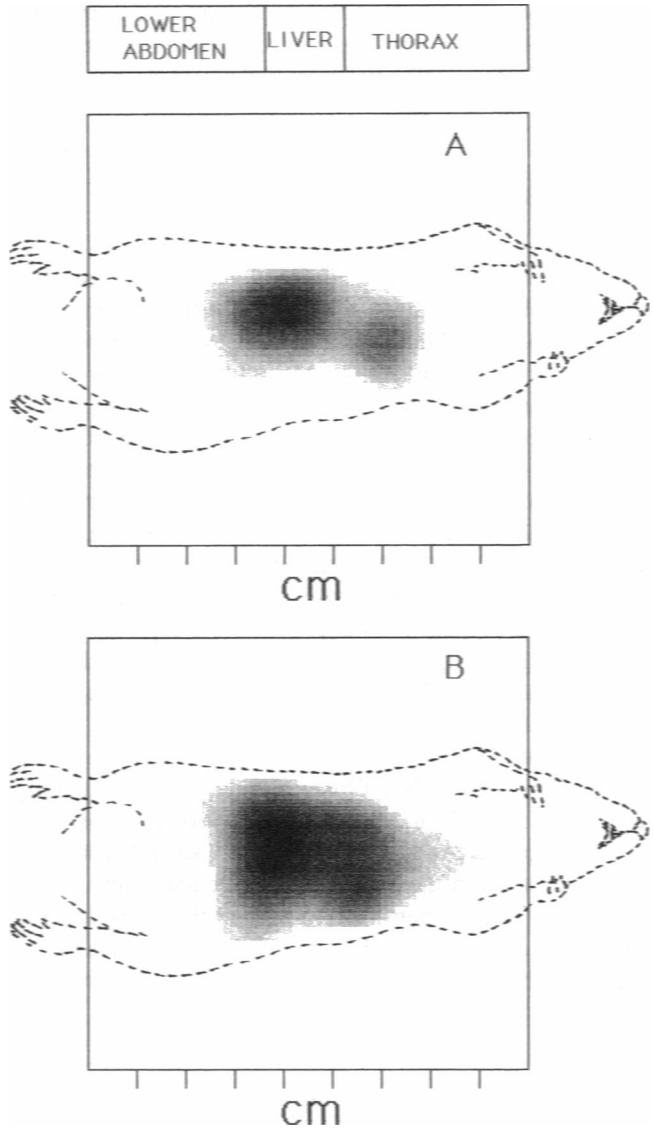

FIGURE 4 2-D images on the longitudinal plane of a rat body obtained at 7 min (*A*) and 17 min (*B*) after PCA administration (4 mmol/kg). The collection time for each image was 5 min. The images (9 × 9 cm) were obtained with an interpolation procedure that gives 64 × 64 pixels, and the signal was scaled with 16 gray levels. The liver region was localized by a DPPH reference. The animal contour was inserted for graphical purposes only.

liver. However, two nuclear magnetic resonance studies (Gallez et al., 1993; Grodd et al., 1987) found that, using similar PCA doses, maximum enhancement in the kidney occurred at 5 and 15 min after the injection. This could explain the PCA signal in the abdominal area corresponding to the kidneys (Fig. 4 *B*). However, the modest resolution of our apparatus does not allow the identification of the organs enhanced in the lower abdomen region. The combination of our EPRI method with a new straightforward magnetic resonance imaging method utilizing susceptibility effects (Bacic et al., 1993) could provide a better understanding of in vivo PCA distribution. An increase of EPRI resolution and/or sensitivity is expected with the use of narrow linewidth probes.

Perdeuterated probes, presently developed in the framework of proton electron double resonance imaging (Lurie et al., 1990), have a linewidth of about 0.003 mT at the tissue oxygen concentration (Andersson et al., 1990).

CONCLUSIONS

This study shows that the use of EPRI provides an opportunity to gain new insight into the spatial distribution of a free radical in selected regions of the rat at different times.

Despite the actual limitations of the sensitivity of the spectrometer without gradient (44 μM) and the spatial resolution of the 2-D images (8 mm), a good enhancement of the liver was obtained by our apparatus with 3–4 mmol/kg PCA. An increase in sensitivity would eventually allow the detection of endogenous free radicals with the aid of a spin trapping technique (Halpern et al., 1993; Janzen and Zhang, 1993; Komarov et al., 1993). In addition, the current pharmacological developments lead us to expect a diversification of the types of paramagnetic substances available that are capable of enhancing specific organs (Gallez et al., 1993) and tumor tissues (Brasch, 1992). Time resolution limits the applicability of our EPRI technique. At the present stage, the acquisition time for 1-D projections is about 50 s. The ongoing development of RF pulsed EPRI techniques at low frequency (Bourg et al., 1993) and the development of a narrow linewidth spin probe (Andersson et al., 1990) should reduce the acquisition time to the millisecond range and allow the attainment of three-dimensional images of the distribution of paramagnetic species in whole rat. This should increase the number of biophysical problems that could be investigated by EPRI.

We wish to thank Dr. G. Placidi for his assistance in the processing of some imaging data.

This research was supported in part by MURST (40%), INFM, INFN, and PF CNR/ACRO.

REFERENCES

Alecci, M., S. Colacicchi, P. L. Indovina, F. Momo, P. Pavone, and A. Sotgiu. 1990. Three-dimensional in vivo ESR imaging in rats. *Magn. Reson. Imag.* 8:59–63.

Alecci, M., S. Della Penna, A. Sotgiu, and L. Testa. 1992a. R. F. (280 MHz) EPR Imaging of extended samples: apparatus and preliminary results. *Appl. Magn. Reson.* 3:909–915.

Alecci, M., S. Della Penna, A. Sotgiu, L. Testa, and I. Vannucci. 1992b. Electron Paramagnetic Resonance spectrometer for three-dimensional in vivo imaging at very low frequency. *Rev. Sci. Instrum.* 63:4263–4270.

Alecci, M., M. Ferrari, R. Passariello, V. Quaresima, A. Sotgiu, and C. L. Ursini. 1992c. Electron paramagnetic resonance imaging of water soluble nitroxide free radical in whole rat. Abstract of the Society of Magnetic Resonance in Medicine, 11th Annual Meeting. Berlin, Germany. p. 4110.

Andersson, S., G. Ehnholm, K. Golman, M. Jurjgensen, I. Leunbach, S. Petersson, F. Rise, O. Salo, and S. Vahasalo. 1990. Overhauser MR imaging with agents with different line widths. *Radiology.* 177:246.

Bacic, G., K. J. Liu, J. A. O'Hara, R. D. Harris, K. Szybinski, F. Goda, and H. M. Swartz. 1993. Oxygen tension in a murine tumor: a combined EPR and MRI study. *Magn. Reson. Med.* 30:568–572.

Bacic, G., M. J. Nilges, R. L. Magin, T. Walczak, and H. M. Swartz. 1989. In vivo localized ESR spectroscopy reflecting metabolism. *Magn. Reson. Med.* 10:266–272.

Bennett, H. F., R. D. Brown III, J. F. W. Keana, S. H. Koenig, and H. M. Swartz. 1990. Interactions of nitroxides with plasma and blood: effect on $1/T_1$ of water protons. *Magn. Reson. Med.* 14:40–55.

Berliner, L. J., H. Fujii, X. Wan, and S. J. Lukiewicz. 1987. Feasibility study of imaging a living murine tumor by electron paramagnetic resonance. *Magn. Reson. Med.* 4:380–384.

Bourg, J., M. C. Krishna, J. B. Mitchell, R. G. Tschudin, T. J. Pohida, W. S. Friaup, P. D. Smith, J. Metcalfe, F. Harrington, and S. Subramanian. 1993. Radiofrequency FT EPR spectroscopy and imaging. *J. Mag. Reson. Ser. B.* 102:112–115.

Brasch, R. C. 1992. New directions in the development of MR imaging contrast media. *Radiology.* 183:1–11.

Brivati, J. A., A. D. Stevens, and M. C. R. Symons. 1991. A radiofrequency ESR spectrometer for *in vivo* imaging. *J. Magn. Reson.* 92: 480–489.

Colacicchi, S., M. Ferrari, and A. Sotgiu. 1992. In vivo electron paramagnetic resonance spectroscopy/imaging: first experiences, problems, and perspectives. *Int. J. Biochem.* 24:205–214.

Couet, W. R., U. G. Eriksson, T. N. Tozer, L. D. Tuck, G. E. Wesbey, D. Nitecki, and R. C. Brasch. 1984. Pharmacokinetics and metabolic fate of two nitroxides potentially useful as contrast agents for magnetic resonance imaging. *Pharmacol. Res.* 1:203–209.

Dalal, D. P., S. S. Eaton, and G. R. Eaton. 1981. The effects of lossy solvents on quantitative EPR studies. *J. Magn. Reson.* 44:415–428.

Froncisz, W., and J. S. Hyde. 1982. The loop-gap resonator: a new microwave lumped circuit ESR sample structure. *J. Magn. Reson.* 47:515–521.

Gadian, D. G., and F. N. H. Robinson. 1979. Radiofrequency losses in NMR experiments on electrically conducting samples. *J. Magn. Reson.* 34:449–455.

Gallez, B., R. Debuyst, R. Demeure, F. Dejehet, C. Grandin, B. Van Beers, H. Taper, J. Pringot, and P. Dumont. 1993. Evaluation of a nitroxyl fatty acid as liver contrast agent for magnetic resonance imaging. *Magn. Reson. Med.* 30:592–599.

Grodd, W., H. Paajanen, U. G. Eriksson, D. Revel, F. Terrier, and R. C. Brasch. 1987. Comparison of ionic and non-ionic spin labels for urographic enhancement in magnetic resonance imaging. *Acta Radiol.* 28: 593–600.

Halpern, H. J., M. Peric, T. D. Nguyen, M. K. Bowman, Y. J. Lin, and B. A. Teicher. 1991. *In vivo* O_2 sensitive imaging at low frequencies. *Phys. Med.* 7:39–45.

Halpern, H. J., S. Pou, M. Peric, C. Yu, E. Barth, and G. M. Rosen. 1993. Detection and imaging of oxygen-centered free radicals with low-frequency electron paramagnetic resonance and signal-enhancing deuterium-containing spin traps. *J. Am. Chem. Soc.* 115:218–223.

Halpern, H. J., D. P. Spencer, J. van Polen, M. K. Bowman, A. C. Nelson, E. M. Dowey, and B. A. Teicher. 1989. Imaging radio frequency electron-spin-resonance spectrometer with high resolution and sensitivity for in vivo measurements. *Rev. Sci. Instrum.* 60:1040–1050.

Hoult, D. I., and P. C. Lauterbur. 1979. The sensitivity of the Zeugmatographic experiment involving human samples. *J. Magn. Reson.* 34: 425–433.

Iannone, A., A. Tomasi, V. Vannini, and H. M. Swartz. 1990. Metabolism of nitroxide spin labels in subcellular fractions of rat liver. II Reduction in the cytosol. *Biochim. Biophys. Acta.* 1034:290–293.

Ishida, H., S. Matsumoto, H. Yokoyama, N. Mori, H. Kumashiro, N. Tsuchihashi, T. Ogata, M. Yamada, M. Ono, T. Kitajima, H. Kamada, and E. Yoshida, 1992. An ESR-CT imaging of the head of a living rat receiving an administration of a nitroxide radical. *Magn. Reson. Imag.* 10: 109–114.

Janzen, E. D., and Y. Zhang. 1993. EPR spin trapping alkoxyl radicals with 2-substituted 5:5-dimethylpyrroline-N-oxides (2-XM_2PO's). *J. Magn. Reson. Ser. B.* 101:91–93.

Komarov, A., D. Mattson, M. M. Jones, P. K. Singh, and C. S. Lai. 1993. In vivo spin trapping of nitric oxide in mice. *Biochem. Biophys. Res. Commun.* 195:1191–1198.

Lebedev, Ya. S., and O. Ye. Yakimchemko. 1991. Magnetic field distributions. *In* EPR Imaging and in vivo EPR. G. R. Eaton, S. S. Eaton, and K. Ohno, editors. CRC Press, Boca Raton, FL. 251–259.

Lurie, D. J., I. Nicholson, M. A. Foster, and J. R. Mallard. 1990. Free radicals imaged in vivo in the rat by using proton-electron double-resonance imaging. *Phil. Trans. R. Soc. Lond. A.* 333:453–456.

Marshall, S. A., B. H. Suits, M. T. Umlor, and Y. N. Zhang. 1988. Imaging electromagnetic fields using the magnetic resonance absorption spectrum of a paramagnetic gas. *J. Magn. Reson.* 76:494–503.

Momo, F., S. Colacicchi, and A. Sotgiu. 1993. Limits of deconvolution in enhancing the resolution in EPR imaging experiments. *Meas. Sci. Technol.* 4:60–64.

Ogata, T., Y. Ishikawa, M. Ono, and L. J. Berliner. 1992. Visualization of eddy-current losses in L-band ESR imaging. *J. Magn. Reson.* 97: 616–622.

Ohno, K., G. R. Eaton, and S. S. Eaton. 1991. The scope of EPR imaging. *In* EPR Imaging and in vivo EPR. G. R. Eaton, S. S. Eaton, and K. Ohno, editors. CRC Press, Boca Raton, FL. 3–8.

Quaresima, V., M. Alecci, M. Ferrari, and A. Sotgiu. 1992. Whole rat paramagnetic resonance imaging of a nitroxide free radical by a radiofrequency (280 MHz) spectrometer. *Biochem. Biophys. Res. Commun.* 183:829–835.

Quaresima, V., C. L. Ursini, G. Gualtieri, A. Sotgiu, and M. Ferrari. 1993. Oxygen-dependent reduction of a nitroxide free radical by electron paramagnetic resonance monitoring of circulating rat blood. *Biochim. Biophys. Acta.* 1182:115–118.

Sotgiu, A. 1985. Resonator design for *in-vivo* ESR spectroscopy. *J. Magn. Reson.* 65:206–214.

Swartz, H. M., and J. F. Glockner. 1991. Measurement of oxygen by EPRI and EPRS. *In* EPR Imaging and in vivo EPR. G. R. Eaton, S. S. Eaton, and K. Ohno, editors. CRC Press, Boca Raton, FL. 261–290.

Takeshita, K., H. Utsumi, and A. Hamada. 1991. ESR measurement of radical clearance in lung of whole mouse. *Biochem. Biophys. Res. Commun.* 177:874–880.